UC Irvine
UC Irvine Previously Published Works

Title

In vivo early detection of smoke-induced airway injury using three-dimensional swept-source optical coherence tomography

Permalink

https://escholarship.org/uc/item/2b89z66p

Journal

Journal of Biomedical Optics, 14(6)

ISSN

1083-3668

Authors

Yin, Jiechen
Liu, Gangjun
Zhang, Jun
et al.

Publication Date

2009

DOI

10.1117/1.3268775

Copyright Information

This work is made available under the terms of a Creative Commons Attribution License, available at https://creativecommons.org/licenses/by/4.0/

Peer reviewed

In vivo early detection of smoke-induced airway injury using three-dimensional swept-source optical coherence tomography

Jiechen Yin,[a] **Gangjun Liu,**[b] **Jun Zhang,**[b] **Lingfeng Yu,**[b] **Sari Mahon,**[b] **David Mukai,**[b] **Matthew Brenner,**[b,c] **and Zhongping Chen**[a,b,*]

[a]University of California, Irvine, Department of Biomedical Engineering, Irvine, California 92697
[b]University of California, Irvine, Beckman Laser Institute, 1002 Health Sciences Road East, Irvine, California 92612
[c]University of California, Irvine Medical Center, Pulmonary and Critical Care Division, Orange, California 92868

Abstract. We report on the feasibility of rapid, high-resolution, 3-D swept-source optical coherence tomography (SSOCT) to detect early airway injury changes following smoke inhalation exposure in a rabbit model. The SSOCT system obtains 3-D helical scanning using a microelectromechanical system motor-based endoscope. Real-time 2-D data processing and image display at the speed of 20 frames/s are achieved by adopting the technique of parallel computing. Longitudinal images are reconstructed via an image processing algorithm to remove motion artifacts caused by ventilation and pulse. Quantitative analyses of tracheal airway thickness as well as thickness distribution along tracheal circumference are also performed based on the comprehensive 3-D volumetric data. © *2009 Society of Photo-Optical Instrumentation Engineers.*
[DOI: 10.1117/1.3268775]

Acute airway injury induced by smoke inhalation is a major cause of morbidity and mortality among victims of fires.[1] There is a major need for the development of new methods for detection and quantitation of the degree of inhalation airway injury at early stages since airway compromise may cause fatal airway obstruction, may be difficult to detect clinically, and may be delayed for days after smoke exposure, making it difficult to manage patients with inhalation injury.[2] Early-stage pathological changes in the airway, such as swelling of the mucosal layer, may be indicative of the extent of injury. Furthermore, minimally invasive techniques that can repeatedly assess airway injury following exposure may provide essential information to determine which patients will require interventions, such as intubation and mechanical ventilation. However, there are no clinically available techniques
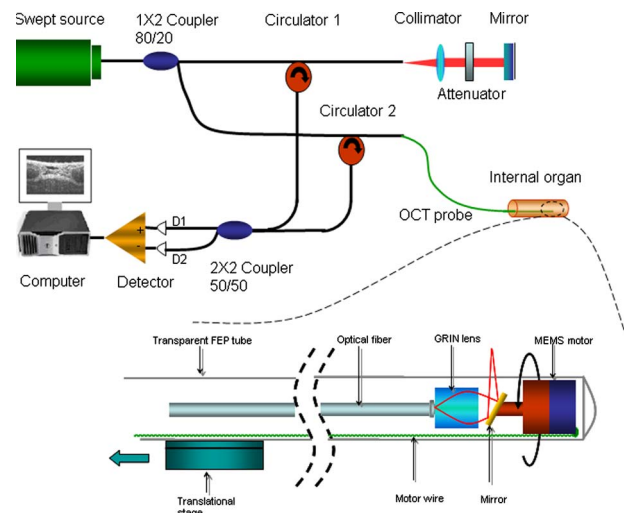
Fig. 1 Schematic of the swept-source OCT (SSOCT) system and MEMS probe.

that are capable of detecting these early pathological changes or following the extent and progression of injury over time after smoke inhalation exposure.

Optical coherence tomography (OCT) is an emerging non-invasive imaging technique that offers high-resolution cross-sectional images of biological tissue *in vivo*.[3] Comprehensive 3-D volumetric data offer promise to provide even more morphological information than 2-D images, and successful 3-D *in vivo* imaging of biological tissue has been reported.[4–6] Previous OCT airway injury studies have demonstrated OCT's capability for distinguishing the changes in airway mucosal thickness.[7] However, since a linear time-domain OCT probe was used in the previous studies, only one 2-D longitudinal image obtained at a specific plane could be acquired at one time, and it was extremely difficult for physicians to know and control the imaging orientation plane and site precisely. Since the distribution of swelling in trachea and bronchi is not uniform, complete 3-D volumetric data that reveal the overall information is of critical importance.

To obtain 3-D volumetric images of the airway, a microelectromechanical systems (MEMS) motor-based probe was used to perform circumferential scanning.[6] The probe was pulled back by a translational stage (Newport Instruments); thus, 3-D helical scanning was achieved. The major optical components were a gradient index (GRIN) lens (1.3 mm in diameter) and a gold-coated mirror, which was attached to the 45-deg-polished motor shaft. Light from a single-mode fiber was focused by the GRIN lens and reflected to tissue by the mirror. The MEMS rotational motor has a diameter of 1.5 mm and a length of 9.4 mm. The outer diameter of the whole packaged probe is 2.2 mm with a rigid distal end approximately 11 mm long (Fig. 1). The motor rotational speed was set to 20 rev/s and synchronized with the speed of our OCT system. The MEMS probe was placed at the approximate center of the trachea in a noncontact mode (confirmed by real-time 2-D images).

In our OCT system (Fig. 1), light from a swept source (center wavelength 1310 nm, FWHM bandwidth 100 nm,

*Tel: 949-824-1247; Fax: 949-824-8413; E-mail: z2chen@uci.edu.

output power 5 mW, scanning rate 20 kHz; Santec Corporation, Komaki, Aichi, Japan) was split by an 80/20 1×2 coupler with 80% of the power directed to the sample arm and the remaining 20% to the reference arm. Two circulators in both arms were used to redirect backscattered and back-reflected light to the two input ports of a 50/50 2×2 coupler for balanced detection. The sensitivity of this system was optimized and measured to be 107 dB. The axial scanning range of this system was 2.9 mm with a 6-dB roll-off at the depth of 2.2 mm. The axial and lateral resolutions of our OCT system in air were 8 and 20 μm, respectively. Dispersion caused by the optical components of the MEMS probe was carefully corrected using a dispersion-compensation algorithm. Real-time 2-D data processing and image display were achieved by adopting the technique of parallel computing in the OCT program we developed. During the experiment, a 12-mm-long section of the trachea was scanned within about 20 s, and 400 B-scans (1024×512 pixels) with interval separation of 30 μm were computed and displayed in real time. Animal handling procedures were similar to those described in our previous work.[7] OCT images of the trachea were taken before and at 2 hours postexposure, as previously described.[7]

Airway thickness could be easily determined at the region where C-shaped cartilage rings underlie the tracheal surface, as shown in Fig. 2. The airway layers provide stronger signal intensity because of the higher scattering properties while the underlying cartilage appears as a signal-poor region (nonreflective) since the tissue is relatively homogenous. The characteristics of these tissue types in an OCT image serve as fundamental principles for mucosa layer edge detection and quantitative analysis of its thickness which was achieved by using our home-developed program capable of detecting mucosa edge (red lines in Fig. 2) and calculating its thickness distribution along the tracheal circumference. In the major part of our algorithm, the 2-D image was scanned column by column for edge point detection. Adaptive thresholds varying according to the average intensity of each column were set to detect each edge point, followed by a polynomial fit to obtain smooth edge surfaces. Errors were calculated, and a criterion was set to eliminate false edge points. This process was repeated several times until errors were less than the preset value to achieve an optimized fit. Finally, the mucosa thickness was obtained simply by computing the distance between the upper and lower edges. Figures 2(a) and 2(b) compare two circumferential B-scan OCT images of the trachea before smoke inhalation and at 2 h postexposure from approximately the same region. The dent artifact was caused by the motor wire within the probe, which blocked the OCT signal. Mucosa layers were outlined using the algorithm already described. Quantitative analysis of average mucosa thickness as well as swelling distribution along the tracheal circumference is depicted in Fig. 2(c). Six entire cartilage rings were covered in the 12-mm-long imaging region, as later shown in Figs. 4(a)–4(c), and six circumferential B-scan images where the mucosa layer is the thinnest above each cartilage ring were selected for average thickness analysis. Taking the center between two cartilaginous-ring margins as the 0-deg point, mucosa layer thickness distributions ranging from 50 to 290 deg were plotted in Fig. 2(c). This angular region was chosen because the C-shaped cartilage rings do not cover the whole 360-deg tracheal circumference, and the polynomial fit at two
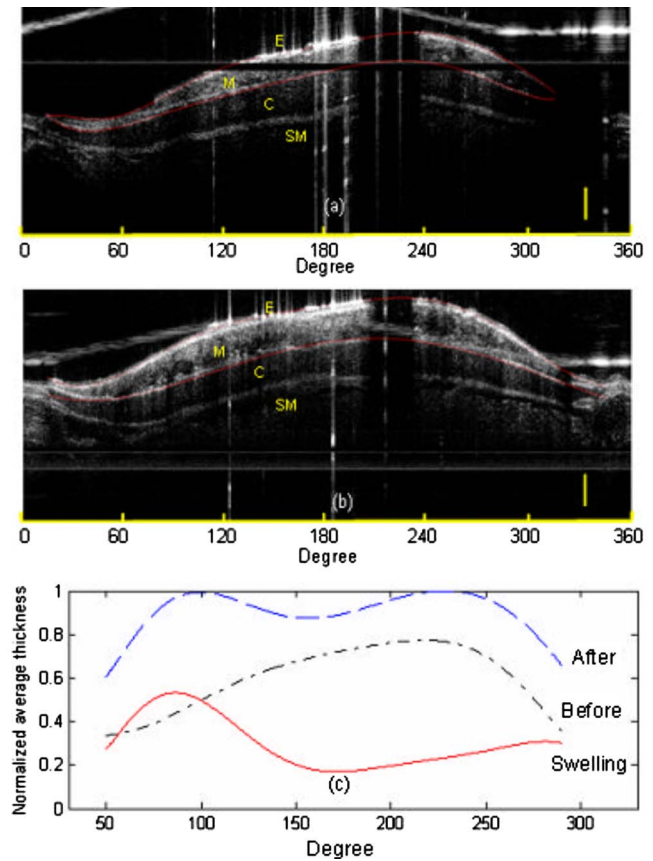
Fig. 2 (a) Baseline and (b) 2-h postexposure circumferential images of rabbit trachea with mucosa layer outlined; (c) normalized average mucosa thickness and swelling distribution along tracheal circumference, calculated based on six characteristic circumferential B-scan images: E, epithelium; M, mucosa; C, cartilage ring; SM, submucosa; scale bar, 500 μm.

margins gives increased error, as one can distinguish from Figs. 2(a) and 2(b). The black dash-dotted line in Fig. 2(c) denotes mucosa thickness measured before smoke inhalation, and the blue dashed line denotes the thickness measured at 2 h postexposure. Swelling was calculated by subtracting the former from the latter, shown as a red solid line. The maximum 53.1% thickening of mucosa layer was found at around 90 deg while the minimum 17.0% thickening was found at around 180 deg. The asymmetric distribution of the calculated swelling was caused by the asymmetric shape of baseline thickness line which probably resulted from the angled circumferential imaging plane and was not ideally perpendicular to the longitudinal axis.

A 3-D reconstruction, as shown in Fig. 3(b), was achieved based on 400 B-scan slices. Images can be reconstructed in any direction based on the 3-D data, and longitudinal OCT images reveal overall airway swelling along the longitudinal direction where the surface-to-cartilage depth could be used as an objective marker for airway thickness. Since the OCT probe was generally in a noncontact mode within the tracheal lumen, motion caused by ventilation and pulse can degrade the quality of the reconstructed image. Figure 4(a) gives an example of this effect. This effect can be corrected by our image reconstruction algorithm, which consists of five main steps: B-scan adjustment, longitudinal reconstruction, surface
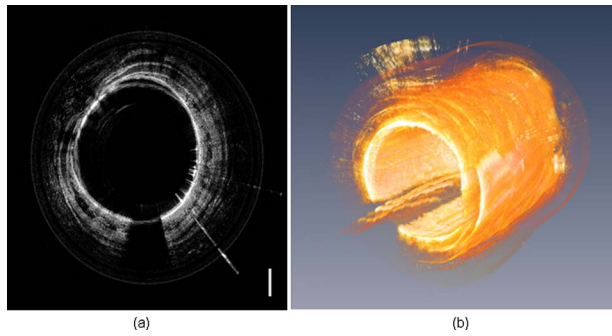
Fig. 3 (a) One slice of rabbit trachea and (b) 3-D reconstruction based on 400 B-scan slices. Scale bar, 500 μm.

detection, polynomial fit, and surface realignment. The first step ensures that each B-scan starts at the same rotational angle. One-row data containing the motor wire as a landmark was extracted from each B-scan image, and then the cross-correlation of two rows from two adjacent B-scans was calculated to determine how many pixels each B-scan should be shifted. Then the initial longitudinal reconstruction at a desired planar angle was performed based on the 3-D data set (where this planar image still contained the motion artifacts). Next, the upper edge of the moving surface was detected through hard thresholding. The corrected smooth surface was
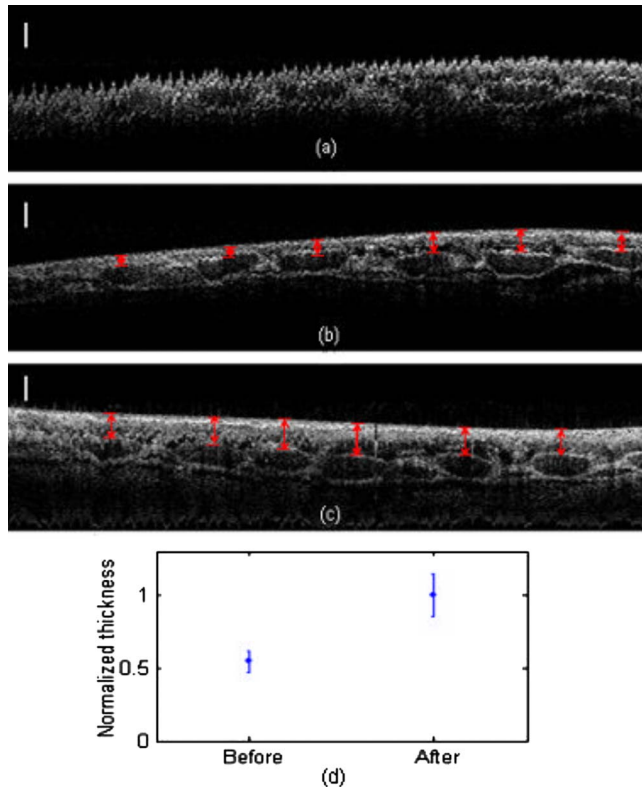
Fig. 4 (a) Initial longitudinal baseline image without motion correction where the cardiac cycle based motion is evident; (b) in contrast, a baseline image with motion artifacts corrected shows improved image quality; (c) 2-h postexposure image with motion artifacts corrected; and (d) normalized average mucosa thickness. Scale bar, 500 μm.

found by a fourth-order polynomial fit of the detected edge curve. Finally, each column of the image was shifted according to the difference between detected surface point and polynomial fit.

Figure 4 demonstrates the longitudinally reconstructed baseline image taken at an $\sim$60-deg angle plane with [Fig. 4(b)] and without [Fig. 4(a)] the realignment algorithm. As we can see, motion artifacts were effectively corrected in Fig. 4(b) compared with those shown in Fig. 4(a). A longitudinally reconstructed image at approximately the same position and angle plane was acquired again 2 h after smoke inhalation and then processed using the same algorithm as shown in Fig. 4(c). Six entire cartilage rings were covered in the 12-mm-long imaging region, and the minimal mucosa thicknesses above these cartilage rings before and 2 h after smoke exposure were studied and are shown in Fig. 4(d). Taking the average mucosa thickness measured at 2 h postexposure as 1, baseline thickness was measured to be 0.543. The standard deviations of mucosa thickness at 2 h exposure and of baseline are 13.2% and 14.9%, respectively.

This study demonstrated the feasibility of a 3-D MEMS motor-based swept-source OCT (SSOCT) endoscope system for detection and assessment of early airway injury induced by smoke inhalation. Image reconstruction along the desired directions and quantitative analysis of smoke-induced airway thickening were obtained based on the comprehensive 3-D volumetric data. The ability to detect and measure early inhalation airway injury using minimally invasive 3-D SSOCT may provide a valuable tool for assessing extent of injury, impending airway obstruction, triage and prognosis, as well as accurate assessment of response to therapy.

References

1. D. N. Herndon, R. E. Barrow, H. A. Linares, R. L. Rutan, T. Prien, L. D. Traber, and D. L. Traber, "Inhalation injury in burned patients: effects and treatment," *Burns Incl Therm Inj* **14**(5), 349–356 (1988).
2. R. H. Demling, "Smoke inhalation injury," *Postgrad Med.* **82**(1), 63–68 (1987).
3. D. Huang, E. A. Swanson, C. P. Lin, J. S. Schuman, W. G. Stinson, W. Chang, M. R. Hee, T. Flotte, K. Gregory, C. A. Puliafito, and J. G. Fujimoto, "Optical coherence tomography," *Science* **254**, 1178–1181 (1991).
4. S. H. Yun, G. J. Tearney, B. J. Vakoc, M. Shishkov, W. Y. Oh, A. E. Desjardins, M. J. Suter, R. C. Chan, J. A. Evans, I.-K. Jang, N. S. Nishioka, J. F. de Boer, and B. E. Bouma, "Comprehensive volumetric optical microscopy *in vivo*," *Nat. Med.* **12**, 1429–1433 (2006).
5. D. C. Adler, Y. Chen, R. Huber, J. Schmitt, J. Connolly, and J. G. Fujimoto, "Three-dimensional endomicroscopy using optical coherence tomography," *Nat. Photonics* **1**, 709–716 (2007).
6. J. Su, J. Zhang, L. Yu, H. G. Colt, M. Brenner, and Z. Chen, "Real-time swept source optical coherence tomography imaging of the human airway using a microelectromechanical system endoscope and digital signal processor," *J. Biomed. Opt.* **13**, 030506 (2008).
7. M. Brenner, K. Kreuter, J. Ju et al., "*In vivo* optical coherence tomography detection of differences in regional large airway smoke inhalation induced injury in a rabbit model," *J. Biomed. Opt.* **13**, 034001 (2008).